A PALMPRINT RECOGNITION ALGORITHM USING PRINCIPAL COMPONENT ANALYSIS OF PHASE INFORMATION

Satoshi Iitsuka, Kazuyuki Miyazawa and Takafumi Aoki

Graduate School of Information Sciences, Tohoku University,
Sendai-shi 980-8579, Japan
E-mail: iitsuka@aoki.ecei.tohoku.ac.jp

ABSTRACT

This paper presents a palmprint recognition algorithm using Principal Component Analysis (PCA) of phase information in 2D (two-dimensional) Discrete Fourier Transforms (DFTs) of palmprint images. To achieve highly robust palmprint recognition, the proposed algorithm (i) limits the frequency bandwidth, and (ii) averages phase spectra using multiple palmprint images captured from the same hand at an enrollment stage. Through a set of experiments, we demonstrate that the proposed method can significantly reduce computational cost without sacrificing recognition performance compared with our previous work using Phase-Only Correlation (POC) — an image matching technique using the phase components in 2D DFTs of given images. Also, the resulting performance is much higher than those of conventional palmprint recognition algorithms which apply PCA to palmprint images, or phase spectra directly.

Index Terms— palmprint recognition, phase information, principal component analysis, biometrics

1. INTRODUCTION

Biometric authentication has been receiving extensive attention over the past decade with increasing demands in automated personal identification. Among many biometrics techniques, palmprint recognition is one of the most reliable approaches, since a palmprint contains many features such as principle lines, ridges, minutiae points, singular points and texture, and is expected to be more distinctive than a fingerprint [1].

We have proposed palmprint recognition algorithms using Phase-Only Correlation (POC) — an image matching technique using the phase components in 2D Discrete Fourier Transforms (DFTs) of given images [2, 3]. These algorithms have efficient recognition performance compared with a Gabor feature-based algorithm [4]. However, high computational cost due to numerous calculations of 2D DFTs can be a drawback of POC-based method when we identify an input palmprint image from a huge database.

Addressing the problem, this paper proposes a palmprint recognition algorithm which performs Principal Component Analysis (PCA) on Fourier phase information of the palmprint images. Instead of applying PCA to phase spectra directly [5], the proposed algorithm (i) limits the frequency bandwidth, and (ii) averages phase spectra using multiple palmprint images captured from the same hand at an enrollment stage. These two techniques have an important role in eliminating meaningless frequency components which degrade recognition performance, and make possible to achieve highly robust palmprint recognition. Through a set of experiments, we demonstrate that the proposed method can significantly reduce computational cost without sacrificing recognition performance compared with the POC-based algorithms. Also, the resulting performance is much higher than those of conventional palmprint recognition algorithms which apply PCA to palmprint images [6], or phase spectra directly [5].

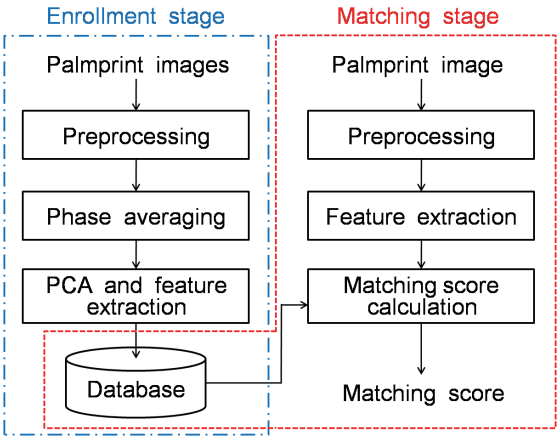

Fig. 1. Flow diagram of the proposed algorithm.

2. ENROLLMENT STAGE

The proposed algorithm consists of the enrollment stage and the matching stage (as illustrated in Fig. 1). This section describes the enrollment stage which consists of (i) preprocessing, (ii) phase averaging and (iii) PCA and feature extraction. We assume that multiple palmprint images are captured from the same hand at this stage.

2.1. Preprocessing

The preprocessing has three steps as follows:

1. A *palmprint region* is extracted from each original palmprint image. In order to extract the center part of palmprint for accurate matching, we employ the method described in [4]. This method defines the *palmprint region* as shown in Fig. 2 (a). We can normalize the rotation by using gaps between fingers as reference points. Fig. 2 (b) shows the extracted palmprint region, where the size of palmprint region is 128×128 pixels in this paper.

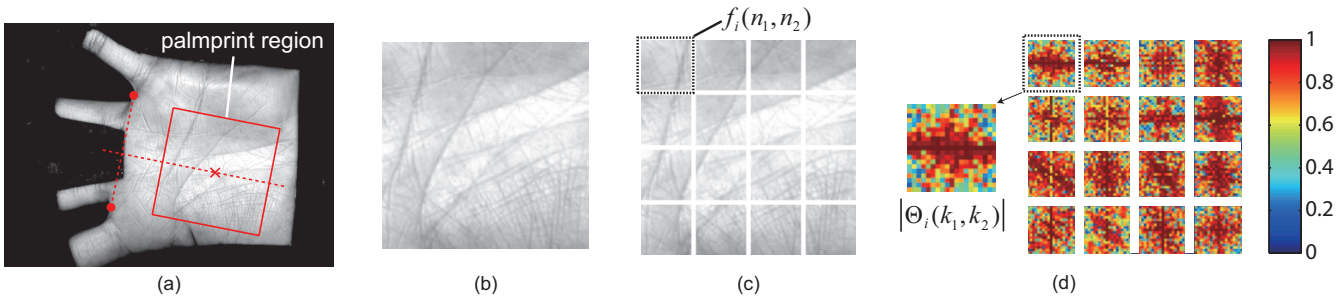

Fig. 2. Enrollment stage: (a) input palmprint image (384 × 284 pixels) and extracted palmprint region (128 × 128 pixels), (b) extracted palmprint region, (c) local block images $f_i(n_1, n_2)$, (d) absolute value of averaged phase $|\Theta_i(k_1, k_2)|$.

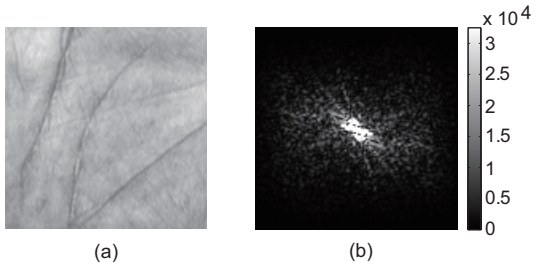

Fig. 3. Amplitude characteristic of extracted palmprint region: (a) extracted palmprint region, (b) amplitude spectrum (the center is zero frequency component).

2. Nonlinear distortion may occur among palmprint images captured at different time. To approximate such distortion by the translational displacement, we divide the extracted palmprint region into multiple small blocks. Assume that the size of a block is $B_1 \times B_2$ pixels. Let $f_i(n_1, n_2)$ be one image block extracted from the palmprint region (see Fig. 2 (c)), where the index ranges are $n_1 = -M_1, \cdots, M_1$ $(M_1 > 0)$, $n_2 = -M_2, \cdots, M_2$ $(M_2 > 0)$ for mathematical simplicity, and, hence $B_1 = 2M_1 + 1$, $B_2 = 2M_2 + 1$. In our experiments, $B_1 = B_2 = 32$. Also, $i = 1, \cdots, P$ is index of registered person, and P is the number of persons in the database. The following steps including Section **2.2** and Section **2.3** are repeated for each block position.

3. This step first aligns the translational displacements among the image blocks extracted from the same position of a series of palmprint images of the same person, then, calculates the 2D DFTs of each block. The translational displacement can be estimated using POC function [7]. Our observation shows that the 2D DFT of a palmprint image contains meaningless high frequency components as shown in Fig. 3. We can improve the matching performance by eliminating the high frequency components. Let $F_i(k_1, k_2)$ denote the band-limited frequency spectrum of $f_i(n_1, n_2)$. $F_i(k_1, k_2)$ is given by

$$\begin{aligned} F_i(k_1, k_2) &= \sum_{n_1=-M_1}^{M_1} \sum_{n_2=-M_2}^{M_2} f_i(n_1, n_2) W_{B_1}^{k_1 n_1} W_{B_2}^{k_2 n_2} \\ &= A_{F_i}(k_1, k_2) \exp\left(j\theta_{F_i}(k_1, k_2)\right), \end{aligned} \quad (1)$$

where $k_1 = -K_1, \cdots, K_1$ $(0 < K_1 \leq M_1)$, $k_2 = -K_2, \cdots, K_2$ $(0 < K_2 \leq M_2)$, $W_{B_1} = \exp(-j2\pi/B_1)$, and $W_{B_2} = \exp(-j2\pi/B_2)$. $A_{F_i}(k_1, k_2)$ is amplitude component and $\theta_{F_i}(k_1, k_2)$ is phase component. Thus, the effective size of frequency spectrum is given by $L_1 = 2K_1 + 1$, $L_2 = 2K_2 + 1$.

2.2. Phase averaging

The meaningless frequency components are not completely eliminated by only limiting the frequency band as Eq. (1). Phase components in low-S/N frequency band behave like random noise. To suppress such unreliable phase components, we take an average of the phase components $\exp(j\theta_{F_i}(k_1, k_2))$ across multiple palmprint images captured from the same hand. The average is calculated using the image blocks extracted from the same position of each palmprint image. Let $\Theta_i(k_1, k_2)$ denote the averaged phase. Absolute values of averaged phase $\Theta_i(k_1, k_2)$ shown in Fig. 2 (d) demonstrate that the meaningless phase components are reduced to almost zero.

2.3. PCA and feature extraction

This step is to extract feature vectors corresponding to individual palmprints using PCA of averaged phase $\Theta_i(k_1, k_2)$. The following describes the details of this step.

1. Let $\psi(k_1, k_2)$ and $\Phi_i(k_1, k_2)$ denote the averaged value of $\Theta_i(k_1, k_2)$ calculated across all persons in the database, and the difference between $\Theta_i(k_1, k_2)$ and $\psi(k_1, k_2)$, respectively. $\psi(k_1, k_2)$ and $\Phi_i(k_1, k_2)$ are given by

$$\psi(k_1, k_2) = \frac{1}{P} \sum_{i=1}^{P} \Theta_i(k_1, k_2), \quad (2)$$

$$\Phi_i(k_1, k_2) = \Theta_i(k_1, k_2) - \psi(k_1, k_2). \quad (3)$$

2. The covariance matrix $\boldsymbol{C}$ is given by

$$\boldsymbol{C} = \sum_{i=1}^{P} \boldsymbol{\Phi}_i \left[\boldsymbol{\Phi}_i\right]^T, \quad (4)$$

where $\boldsymbol{\Phi}_i$ is the $L_1 \cdot L_2 \times 1$ vector, corresponding to the $L_1 \times L_2$ matrix $\Phi_i(k_1, k_2)$. We compute eigenvalues and eigenvectors. Let the dth largest eigenvalue be denoted by λ_d, and the eigenvector corresponding to λ_d be denoted by $\boldsymbol{u}_d$.

3. We reduce the dimensionality of an eigenspace from $L_1 \cdot L_2$ to D by taking only D eigenvectors corresponding to largest D eigenvalues. A feature vector $\boldsymbol{\Omega}_i$ is given by

$$\boldsymbol{\Omega}_i = [\omega_{i,1}, \omega_{i,2}, \cdots, \omega_{i,D}]^T, \quad (5)$$

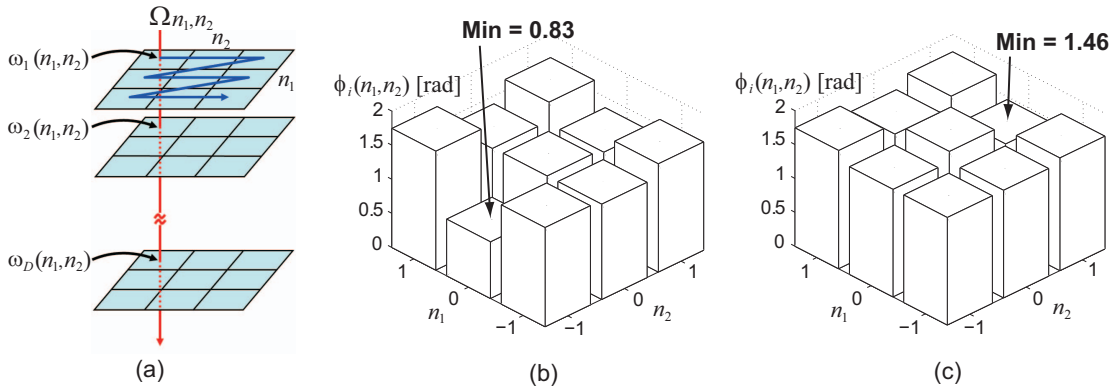

Fig. 4. Matching stage: (a) feature vector generation, (b) $\phi_i(n_1, n_2)$ in genuine matching, (c) $\phi_i(n_1, n_2)$ in impostor matching.

$$\omega_{i,d} = \frac{\langle \overline{\boldsymbol{u}_d}, \boldsymbol{\Phi}_i \rangle}{L_1 L_2}, \tag{6}$$

where $d = 1, \cdots, D$, and $\langle ., . \rangle$ denotes inner product. $\overline{\boldsymbol{u}_d}$ is the complex conjugate of $\boldsymbol{u}_d$. The averaged value $\psi(k_1, k_2)$, the eigenvector $\boldsymbol{u}_d$, and the feature vector $\boldsymbol{\Omega}_i$ are enrolled in the database.

3. MATCHING STAGE

This section describes the matching stage which consists of (i) preprocessing, (ii) feature extraction and (iii) matching score calculation. The details of each step are described in the following.

3.1. Preprocessing

This step is performed in much the same way as that of the enrollment stage described in Section **2.1**.

1. A palmprint region is extracted from an input palmprint image.
2. The palmprint region is divided into multiple small blocks. The size of a block is $B_1 \times B_2$ pixels. Let $g(n_1, n_2)$ be one image block extracted from the palmprint region. The following steps including Section **3.2** are repeated for each block.
3. Let $G(k_1, k_2)$ denote the band-limited frequency spectrum of $g(n_1, n_2)$. $G(k_1, k_2)$ is given by

$$\begin{aligned} G(k_1, k_2) &= \sum_{n_1=-M_1}^{M_1} \sum_{n_2=-M_2}^{M_2} g(n_1, n_2) W_{B_1}^{k_1 n_1} W_{B_2}^{k_2 n_2} \\ &= A_G(k_1, k_2) \exp\left(j\theta_G(k_1, k_2)\right), \end{aligned} \tag{7}$$

where $A_G(k_1, k_2)$ is amplitude component and $\theta_G(k_1, k_2)$ is phase component.

3.2. Feature extraction

A correlation function is defined for dealing with the translational displacement between image blocks. A feature vector corresponding to the input palmprint image is obtained from the correlation function.

1. Let $\Phi(k_1, k_2)$ denote the difference between $\exp\left(j\theta_G(k_1, k_2)\right)$ and $\psi(k_1, k_2)$ as follows:

$$\Phi(k_1, k_2) = \exp\left(j\theta_G(k_1, k_2)\right) - \psi(k_1, k_2). \tag{8}$$

2. Using 2D inverse DFT, the correlation function $\omega_d(n_1, n_2)$ is defined as

$$\begin{aligned} \omega_d(n_1, n_2) &= \frac{1}{L_1 L_2} \sum_{k_1=-K_1}^{K_1} \sum_{k_2=-K_2}^{K_2} \overline{u_d(k_1, k_2)} \Phi(k_1, k_2) \\ &\quad \times W_{L_1}^{-k_1 n_1} W_{L_2}^{-k_2 n_2}, \end{aligned} \tag{9}$$

where $n_1 = -K_1, \cdots, K_1$, $n_2 = -K_2, \cdots, K_2$, and hence $L_1 = 2K_1 + 1$, $L_2 = 2K_2 + 1$. $u_d(k_1, k_2)$ is the $L_1 \times L_2$ matrix corresponding to the $L_1 \cdot L_2 \times 1$ vector $\boldsymbol{u}_d$.

3. In the case of genuine matching, the feature vector $\boldsymbol{\Omega}_i$ appears on a point in $\omega_d(n_1, n_2)$ which corresponds to the translational displacement between image blocks. (If there is no displacement between the input palmprint image and the images captured in the enrollment stage, the feature vector $\boldsymbol{\Omega}_i$ will appear at the origin, $(n_1, n_2) = (0, 0)$, of $\omega_d(n_1, n_2)$.) We can achieve translation-invariant matching by generating feature vectors from every point of $\omega_d(n_1, n_2)$. A feature vector $\boldsymbol{\Omega}_i$ corresponding to a point (n_1, n_2) is given by

$$\boldsymbol{\Omega}_{n_1,n_2} = \left[\omega_1(n_1, n_2), \omega_2(n_1, n_2), \cdots, \omega_D(n_1, n_2)\right]^T. \tag{10}$$

Fig. 4 (a) shows an example of feature vector generation when $L_1 = L_2 = 3$.

3.3. Matching score calculation

The angle $\phi_i(n_1, n_2)$ between $\boldsymbol{\Omega}_i$ and $\boldsymbol{\Omega}_{n_1,n_2}$ is given by

$$\phi_i(n_1, n_2) = \arccos\left(\frac{\langle \boldsymbol{\Omega}_i, \boldsymbol{\Omega}_{n_1,n_2} \rangle}{||\boldsymbol{\Omega}_i|| ||\boldsymbol{\Omega}_{n_1,n_2}||}\right). \tag{11}$$

The matching score is defined as the average value of a set of minimum values of $\phi_i(n_1, n_2)$ calculated from every block pair. Figs. 4 (b) and (c) show examples of $\phi_i(n_1, n_2)$ in genuine matching and impostor matching, respectively ($L_1 = L_2 = 3$). In the case of genuine matching, the distinctive minimum value can be found in a point corresponding to displacement between image blocks, while, with impostor matching, $\phi_i(n_1, n_2)$ has uniform, large values.

4. EXPERIMENTS AND DISCUSSION

This section describes a set of experiments using the PolyU palmprint database [8] for evaluating the performance of the proposed

Table 1. Experimental results of algorithm (A).

the number of feature dimensions	50	100	150	200	250	300
EER [%]	22.309	21.048	20.652	20.292	20.142	20.135

Table 2. Experimental results of algorithm (C).

the number of feature dimensions	50	100	150	200	250	300
EER [%]	0.628	0.131	0.087	0.065	0.066	0.067
the number of 2D DFTs	816	1,616	2,416	3,216	4,016	4,816

palmprint recognition algorithm. This database consists of 7,752 images (384×284 pixels) with 386 subjects and about 20 different images captured at different times (1st time and 2nd time) of each person. In this paper, we select 300 persons from the database. For each 300 person, we use five images captured at 1st time in the enrollment stage, and use five images captured at 2nd time in the matching stage.

In the experiments, the matching performance is evaluated by the Equal Error Rate (EER), which is defined as the error rate where the False Non-Match Rate (FNMR, the probability that an authorized person is falsely rejected) and the False Match Rate (FMR, the probability that a nonauthorized person is falsely accepted as an authorized person) are equal. We first evaluate the genuine matching score for all the possible combinations of genuine attempts (5×300 = 1,500 attempts). Next, we evaluate the impostor matching score for all the possible combinations of impostor attempts ($5 \times 299 \times 300$ = 448,500 attempts).

We compare three different algorithms: (A) Lu's algorithm which applies PCA to palmprint images [6], (B) the POC-based algorithm [3], (C) the proposed algorithm. Table 1 shows EERs of the algorithm (A) with different feature dimensions. The EER of the POC-based algorithm (B) is 0.013 % and the number of 2D DFTs is 9,916 in the matching stage. Table 2 shows EER and computational cost of 2D DFT calculations (in Eq. (7) and Eq. (9)) in the matching stage of the proposed algorithm (C) when changing the number of feature dimensions D and the bandwidth parameters $K_1/M_1 = K_2/M_2 \simeq 0.6$ ($L_1 = L_2 = 19$). When $D = 200$, the proposed algorithm shows the best recognition performance (EER = 0.065 %, and the number of 2D DFTs is 3,216). The proposed algorithm (C) exhibits better recognition performance, since the EER is very low compared with the conventional algorithm (A). In addition, the proposed algorithm (C) can significantly reduce computational cost without sacrificing recognition performance compared with the POC-based algorithm (B).

Table 3 summarizes the results when the algorithms (A), (B) and (C) show the lowest EERs, respectively. In the proposed algorithm (C), we compare four different cases: (i) with bandlimiting and phase averaging, (ii) with only bandlimiting (and without phase averaging), (iii) with only phase averaging (and without bandlimiting), (iv) without bandlimiting and phase averaging [5]. As is observed in Table 3, limiting the frequency bandwidth and averaging phase components play an important role in improving recognition performance.

5. CONCLUSION

This paper proposed a palmprint recognition algorithm using Principal Component Analysis (PCA) of phase information. Limiting the frequency band and averaging phase spectra can reduce harmful effects of meaningless high frequency components. Experimental evaluation demonstrates that the proposed method can significantly reduce computational cost without sacrificing recognition performance compared with our previous work using Phase-Only Correlation (POC). Also, the resulting performance is much higher than those of conventional palmprint recognition algorithms which apply PCA to palmprint images, or phase spectra directly.

Table 3. Summary of results.

Algorithm		EER [%]	the number of 2D DFTs
(A)		20.135	—
(B)		0.013	9,916
(C)	(i)	0.065	3,216
	(ii)	0.166	3,216
	(iii)	0.212	3,216
	(iv)	1.670	3,216

6. REFERENCES

[1] D. Zhang, *Palmprint Authentication*, Kluwer Academic Publication, 2004.

[2] K. Ito, T. Aoki, H. Nakajima, K. Kobayashi, and T. Higuchi, "A palmprint recognition algorithm using phase-only correlation," *IEICE Trans. Fundamentals*, vol. E91-A, no. 4, pp. 1023–1030, Apr. 2008.

[3] S. Iitsuka, K. Ito, and T. Aoki, "A practical palmprint recognition algorithm using phase information," *Proc. 19th Int. Conf. Pattern Recognition*, Dec. 2008.

[4] D. Zhang, W.-K. Kong, J. You, and M. Wong, "Online palmprint identification," *IEEE Trans. Pattern Anal. Machine Intell.*, vol. 25, no. 9, pp. 1041–1050, Sep. 2003.

[5] M. Savvides, B.V.K. Vijaya Kumar, and P.K. Khosla, "Eigenphases vs. eigenfaces," *Proc. 17th Int. Conf. Pattern Recognition*, vol. 3, pp. 810–813, Aug. 2004.

[6] G. Lu, D. Zhang, and K. Wang, "Palmprint recognition using eigenpalms features," *Pattern Recognition Letters*, vol. 24, pp. 1463–1467, Aug. 2003.

[7] K. Takita, T. Aoki, Y. Sasaki, T. Higuchi, and K. Kobayashi, "High-accuracy subpixel image registration based on phase-only correlation," *IEICE Trans. Fundamentals*, vol. E86-A, no. 8, pp. 1925–1934, Aug. 2003.

[8] PolyU Palmprint Database, http://www4.comp.polyu.edu.hk/˜biometrics/.